




Plastid genome insight to the taxonomic problem for *Aconitum pendulum* and *A. flavum* (Ranunculaceae)

Qiang Li^{1,2} · Mingze Xia^{1,2} · Jingya Yu^{1,2} · Shilong Chen¹ · Faqi Zhang^{1,3} 

Received: 5 August 2021 / Accepted: 15 November 2021 / Published online: 10 February 2022
© Plant Science and Biodiversity Centre, Slovak Academy of Sciences 2022

Abstract

As the original species of traditional Chinese medicine “Tie Bang Chui,” the distribution of the *Aconitum pendulum* and *A. flavum* almost wholly overlap. This study compared the complete plastid genome (plastome) of *A. flavum* and *A. pendulum* to assess their phylogenetic relationships. The plastome sizes of *A. flavum* range from 155,642 bp (*A. flavum* MW839582) to 155,717 bp (*A. flavum* MW839579), *A. pendulum* range from 155,667 bp (*A. pendulum* MW839577) to 155,713 bp (*A. pendulum* MW839581). The plastomes are identical, with 131 genes, including eight rRNA genes, 37 tRNA genes, 86 protein-coding genes, and one pseudogene. Long repeats sequences were present in both coding regions and non-coding regions. There were highly variables in the non-coding region both in intra- and interspecies levels. Nine highly variable regions were detected that were suitable for phylogenetic analysis. Moreover, in the protein-coding region, *rpoC1* was more divergent in intraspecies level. Furthermore, protein-coding genes were ideal for species delimitation in *Aconitum* species than highly variated regions. Phylogenetic analysis suggests that individuals of *A. pendulum* and *A. flavum* were not clustered by species. It might be affected by geographical and ecological factors. *A. flavum* and *A. pendulum* have similar morphological characteristics, overlap geographical distribution, highly identical plastome structure, and indistinct phylogenetic relationship. Further research for the two species is necessary, such as population genetic study, to reveal they are the same or two distinct species.

Keywords *Aconitum* · Plastid genome · Phylogeny · Qinghai-Tibetan plateau

Introduction

Genus *Aconitum* (Ranunculaceae) includes more than 400 species, with 211 species distributed in China, 166 of which are endemic, mainly distributed in temperate regions of the northern hemisphere (southwest China and the eastern Himalaya in China) (Li and Kadota 2001). *Aconitum*

has been divided into three subgenera, *Aconitum*. subgenus *Aconitum*, *A.* subgenus *Lycocotonus* and *A.* subgenus *Gymnaconitum* (Tamura 1990; Jabbour and Renner 2012). *Aconitum* originated in Asia subsequently migrated to Europe and North America (Jabbour and Renner 2012). More than 70 *Aconitum* species have been treated as medicine plants, although most are poisonous (Xiao et al. 2006; Ma et al. 2015). *Aconitum* species manifest variable and similar morphologies, making species delimitation difficult (Kita et al. 1995). There are 160 *Aconitum* species available in chromosome number databases (Missouri Botanical Garden, <http://legacy.tropicos.org/Project/IPCN>). *Aconitum* includes diploids, triploids, tetraploids, and hexaploid plants, most of which are diploids (Li et al. 2012). *Aconitum pendulum* Busch and *Aconitum flavum* Hand.-Mazz. are diploids with the chromosome number of $2n = 2x = 16$ (Yang 1994).

A. pendulum and *A. flavum* (Ranunculaceae) are mainly distributed in Qinghai-Tibetan Plateau and its adjacent areas. *A. pendulum* and *A. flavum* are standard Tibetan medicine, mainly used in treating rheumatoid arthritis, traumatic injury,

✉ Shilong Chen
slchen@nwipb.cas.cn

✉ Faqi Zhang
fqzhang@nwipb.cas.cn

¹ Key Laboratory of Adaptation and Evolution of Plateau Biota, Northwest Institute of Plateau Biology, Chinese Academy of Sciences & Institute of Sanjiangyuan National Park, Chinese Academy of Sciences, Xining 810008, China

² University of Chinese Academy of Sciences, Beijing 100049, China

³ Qinghai Provincial Key Laboratory of Crop Molecular Breeding, Xining 810008, China

chilblains, and joint pain (Salick et al. 2006; El-Shazly et al. 2016). More than 42 alkaloids have been found in *A. pendulum*, of which diterpenoid alkaloids, a group of toxic and medicinal constituents such as aconitine. Hypaconitine and aldohypaconite were considered the main active component (Wang et al. 2016; Wang et al. 2019). For the two species, morphological features and ecological niches were highly identical. There were just minor differences in caudex (carrot-shaped vs. obconical), rachis & pedicels (appressed pubescent vs. spreading yellow pubescent), and upper sepal (galeate-navicular vs. navicular-falcate or falcate and clawed). The relationship between *A. pendulum* and *A. flavum* remains controversial. Prior researches demonstrated *A. flavum* was sister to *Aconitum falciforme* Hand.-Mazz. with 87% bootstrap support and the relationship of *A. pendulum* was unresolved based on ITS sequence (Luo et al. 2005). The complete plastome implied that *A. pendulum* was sister to *Aconitum contortum* Finet et Gagnep., *A. flavum* and *Aconitum brachypodum* Diels. clustered into one branch with 100% bootstrap values (Liu et al. 2020; Wang and Li 2020). The seed morphology of the two species belongs to the same type (Kong et al. 2013). Clustering analysis of karyotype resemblance-near coefficient indicated *A. flavum* is close to *Aconitum brunneum* Hand.-Mazz. (Sataloff et al. 2012). Nevertheless, most of the prior researches that not include *A. pendulum* and *A. flavum*.

The plastid genome (plastome) owns a conservative genome structure in land plants, which is composed of two inverted repeats (IR) regions, a large single copy (LSC) region, and a small single copy (SSC) region (Sugiura 1989). There are more than 20 plastomes of *Aconitum* species have been published in NCBI. The plastome length range from 151,214 bp (*Aconitum episcopale* Leveille) to 157,215 bp (*Aconitum sinomontanum* Nakai). There is a small distinguish between *Aconitum* species in plastomes size, structure, and expansion/contraction of IRs (Park et al. 2017). As a super-barcode marker, the plastomes are widely used in phylogeny, species delimitation in closely related species (Chen et al. 2018; Jiang et al. 2020). For example, based on 79 protein-coding genes, phylogenetic analysis of *Lamiaceae* provided new insights into the phylogenetic relationships of a taxonomic category below *Lamiaceae* (Zhao et al. 2021).

We assembled the complete plastomes of *A. pendulum* and *A. flavum* with a total of six individuals to (i) characterize and compare the complete plastome of *A. flavum* and *A. pendulum*, (ii) assess the taxonomic positions and the relationships of *A. pendulum* and *A. flavum*.

Materials and methods

Plant material, DNA extraction, and sequencing

Fresh leaves of *A. flavum* and *A. pendulum* were obtained from different locations in Qinghai Province. All specimens were deposited into the Qinghai-Tibetan Plateau Museum of Biology, Northwest Institute of Plateau Biology, Chinese Academy of Sciences (HNWP). The vouchers' information was presented in Table S1. The silica gel-dried leaves were sent to Novogene Co., Ltd. (Beijing, China) for library construction and sequencing. DNA extracted using cetyltrimethylammonium bromide (CTAB) methods, paired-end reads of 2 × 150 bp for all samples were pooled and run in a single lane on an Illumina NovaSeq 6000 (Illumina Inc., San Diego, CA, USA). Between 0.92 and 2.04 GB paired clean reads were generated. The annotated plastomes were submitted to Genbank through the BankIt platform (<https://www.ncbi.nlm.nih.gov/WebSub/>).

Plastome assembling and annotation

The de novo assembling of the clean read was performed on GetOrganelle pipeline (Jin et al. 2020), and SPAdes were conducted de novo assembly (Bankevich et al. 2012). Bandage (Wick et al. 2015) was used to visualize, label, and check the assembly graph. GeSeq and OrganelleGenomeDRAW (OGDRAW) were used to annotate and visualization the plastome of the two *Aconitum* species (Tillich et al. 2017; Greiner et al. 2019).

Compare and analysis Plastome structure

The complete plastomes of *A. pendulum* and *A. flavum* were compared with other species of Ser. *Brachypoda* downloads from NCBI, including *Aconitum brachypodum* Diels. (NC_041579) and *Aconitum coreanum* (Lévl.) Rapaics (NC_013421). It was performed on the mVISTA program with a shuffle-LAGAN model, and *A. flavum* as a reference (Frazer et al. 2004). The GC content and codon usage of *A. pendulum* and *A. flavum* MW839582 were performed by MEGA X 11.0 (Kumar et al. 2018). The boundaries between the IR and SC regions of eight species were compared and visualized by IRscope (<https://irscope.shinyapps.io/irapp/>). DnaSP v6 was used to determine the average number of nucleotide differences among the 17 *Aconitum* species (Rozas et al. 2017).

Repeat sequences analysis

REPuter program (<https://bibiserv.cebitec.uni-bielefeld.de/reputer>) was performed to infer forward (F), reverse (R), complement (C) and palindrome (P) repeat sequences, with the maximum and minimum repeat size set at 50 and 30, and Hamming distance of 3 (Kurtz et al. 2001).

Phylogenetic analysis

Plastomes of 17 species of *Aconitum* from NCBI (Table S3), *Delphinium grandiflorum* L. (NC_049872), and *Delphinium brunonianum* Royle (NC_051554) were outgroups. The 30 plastome sequences were aligned using MAFFT v.7 (Katoh et al. 2019), and the aligned sequences subsequently were manually adjusted by MEGA X 11.0 (Kumar et al. 2018). Seventy-three protein-coding genes shared by 30 plastome sequences were extracted by PhyloSuit (Zhang et al. 2020). Maximum likelihood (ML) estimation with 1000 bootstrap replications was conducted using IQ-TREE 2 (Minh et al. 2020). The best-fitting models were used ModelFinder in IQ-TREE: for protein-coding genes, TVM + F + G4. For

Bayesian Inference(BI) analysis, MrBayes 3.2.6 (Ronquist et al. 2012) in PhyloSuite was used to BI tree, which under GTR+ G + F model (2 parallel runs, 1 000 000 generations) from ModelFinder.

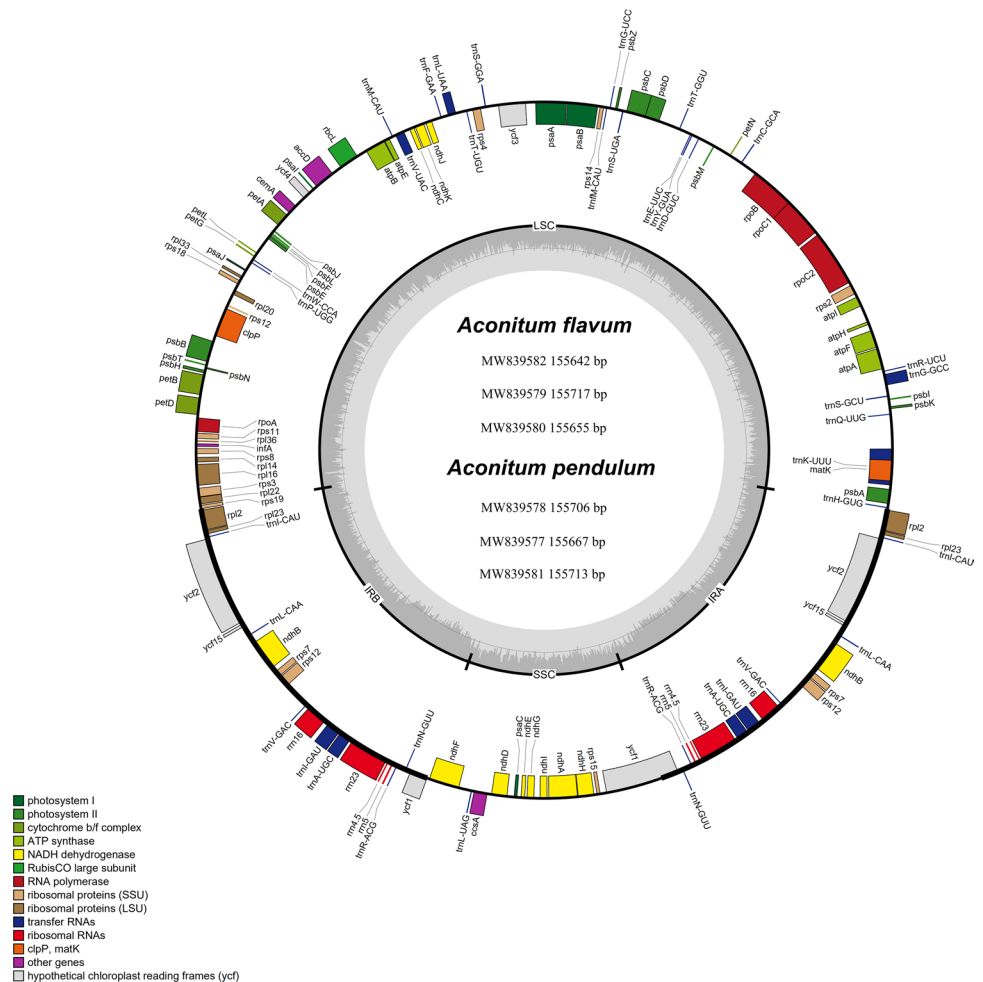
Results

Characterize the complete plastome sequences

We have obtained the NGS clean data ranging from 2.04 GB (*A. flavum* MW839582) to 922.49 MB (*A. flavum* MW839579), the read number with minimum and maximum values of 29 595 524 (*A. flavum* MW839579), and 60 486 426 (*A. flavum* MW839582). Then the two species were de novo assembly using GetOrganelle with K-mer values 21, 45, 65, 85, 105 and using *A. flavum* (MT571464) plastome as a reference.

The plastome sizes of *A. flavum* ranged from 155,642 bp to 155,717 bp, and *A. pendulum* from 155,597 bp to 155,713 bp (Fig. 1). The length of LSC regions in *A. flavum* was 86,281 bp, 86,389 bp, 86,233 bp, and 86,246 bp for the

Fig. 1 Gene maps of the complete chloroplast genomes of *A. flavum* and *A. pendulum*. Genes on the inside are transcribed in a clockwise direction, while genes on the outside are transcribed in a counterclockwise direction



MW839579, MT571464, MW839582, and MW839580. The most extended LSC region in *A. pendulum* was 86,336 bp (*A. pendulum* MN719135), and the shortest was 87,259 bp (*A. pendulum* MW839577). The LSC region has more variation in different individuals than SSC and IR regions, with 156 bp and 77 bp variation among intraspecies in *A. flavum* and *A. pendulum* (Table S2). Overall, the length of plastomes in intraspecies level has a slight difference.

Table 1 Comparison of general characteristics of the plastomes of the three *Aconitum* species

Sequence Region	<i>A. pendulum</i>	<i>A. flavum</i>	<i>A. kusnezoffii</i>
Total size(bp)	155,713	155,642	155,862
LSC size(bp)	86,280	86,233	86,335
SSC size(bp)	17,001	16,977	16,945
IR size(bp)	26,216	26,216	26,291
number of genes	131	131	132
GC content(%)	38.1	38.1	38.1
rRNA gene number	8	8	8
tRNA gene number	37	37	37
Protein-coding gene	86	86	85
Pseudogene	1	1	2

All three species (*A. flavum*, *Aconitum kusnezoffii* Reichb., and *A. pendulum*) share a typical quadripartite structure of plastomes with an LSC, SSC, and two IR regions. *A. pendulum* and *A. flavum* exhibit the same length in two IR regions (26,216 bp). SSC region in *A. pendulum* (17,001 bp) has slightly larger than *A. flavum* (16,977 bp) and *A. kusnezoffii* (16,945 bp). LSC region range from 86,233 bp (*A. flavum*) to 86,335 bp (*A. kusnezoffii*). The GC content of the three *Aconitum* species was 38.1%. While the plastome of *A. pendulum* and *A. flavum* has 131 genes: 8 rRNA genes, 37 tRNA genes, 86 protein-coding genes, and one pseudogene, establishing slightly distinguished from *A. kusnezoffii* (85 protein-coding gene and two pseudogenes) (Table 1). The chloroplast genome of *A. pendulum* and *A. flavum* contained 131 genes, 19 of which are duplicated genes. *ndhB*, *rpl2*, *rpl23*, *rps7*, *rps12*, *ycf2*, and *ycf15* are duplication in 86 CDS genes of *A. pendulum* and *A. flavum* (Table 2).

Repeat sequence analysis

A total of 10 forward repeats, 14 palindromic repeats, three reverse repeats, and one complement repeats were present in the plastome of *A. pendulum*. While the chloroplast of *A. flavum* contained nine forward repeats, 13 palindromic

Table 2 List of genes in the *A. pendulum* and *A. flavum* chloroplast genomes. ^dGenes indicates gene with double

Category	Group of gene	Gene name	
Self-replication	rRNA genes	<i>rrn16^d</i> , <i>rrn23^d</i> , <i>rrn4.5^d</i> , <i>rrn5^d</i>	
	tRNA genes	<i>trnA-UGC^d</i> , <i>trnC-GCA</i> , <i>trnD-GUC</i> , <i>trnE-UUC</i> , <i>trnF-GAA</i> , <i>trnFM-CAU</i> , <i>trnG-GCC</i> , <i>trnG-UCC</i> , <i>trnH-GUG</i> , <i>trnI-CAU^d</i> , <i>trnI-GAU^d</i> , <i>trnK-UUU</i> , <i>trnL-CAA^d</i> , <i>trnL-UAA</i> , <i>trnL-UAG</i> , <i>trnM-CAU</i> , <i>trnN-GUU^d</i> , <i>trnP-UGG</i> , <i>trnQ-UGG</i> , <i>trnR-ACG^d</i> , <i>trnR-UCU</i> , <i>trnS-GCU</i> , <i>trnS-GGA</i> , <i>trnS-UGA</i> , <i>trnS-UGA</i> , <i>trnT-GGU</i> , <i>trnT-UGU</i> , <i>trnV-GAC^d</i> , <i>trn-UAC</i> , <i>trnW-CCA</i> , <i>trnY-GUA</i>	
	Small subunit of ribosome	<i>rps12^d</i> , <i>rps2</i> , <i>rps14</i> , <i>rps4</i> , <i>rps18</i> , <i>rps11</i> , <i>rps8</i> , <i>rps3</i> , <i>rps19</i> , <i>rps7^d</i> , <i>rps15</i>	
	Large subunit of ribosome	<i>rpl33</i> , <i>rpl20</i> , <i>rpl36</i> , <i>rpl14</i> , <i>rpl16</i> , <i>rpl22</i> , <i>rpl2^d</i> , <i>rpl23^d</i>	
	DNA-dependent RNA polymerase	<i>rpoA</i> , <i>rpoC2</i> , <i>rpoC1</i> , <i>rpoB</i>	
	Genes for photosynthesis	Subunits of photosystem I	<i>psaB</i> , <i>psaA</i> , <i>psaI</i> , <i>psaJ</i> , <i>psaC</i>
		Subunits of photosystem II	<i>psbA</i> , <i>psbK</i> , <i>psbI</i> , <i>psbM</i> , <i>psbD</i> , <i>psbC</i> , <i>psbZ</i> , <i>psbJ</i> , <i>psbL</i> , <i>psbF</i> , <i>psbE</i> , <i>psbB</i> , <i>psbT</i> , <i>psbN</i> , <i>psbH</i>
		ATP synthase gene	<i>atpA</i> , <i>atpF</i> , <i>atpH</i> , <i>atpI</i> , <i>atpE</i> , <i>atpB</i>
		Large subunit of rubisco	<i>rbcL</i>
		Subunits of cytochrome b/f complex	<i>petN</i> , <i>petA</i> , <i>petL</i> , <i>petG</i> , <i>petB</i> , <i>petD</i>
Subunit of NADH-dehydrogenase		<i>ndhJ</i> , <i>ndhK</i> , <i>ndhC</i> , <i>ndhB^d</i> , <i>ndhF</i> , <i>ndhD</i> , <i>ndhE</i> , <i>ndhG</i> , <i>ndhI</i> , <i>ndhA</i> , <i>ndhH</i>	
Other genes		Genes of unknown function	<i>ycf1</i> , <i>ycf3</i> , <i>ycf4</i> , <i>ycf2^d</i> , <i>ycf15^d</i>
	Maturase	<i>matK</i>	
	acetyl-CoA carboxylase	<i>accD</i>	
	Envelope membrane protein	<i>cemA</i>	
	cytochrome c biogenesis	<i>ccsA</i>	
	ATP-dependent Clp protease proteolytic subunit	<i>clpP</i>	
	translational initiation factor 1 protein	<i>infA</i>	

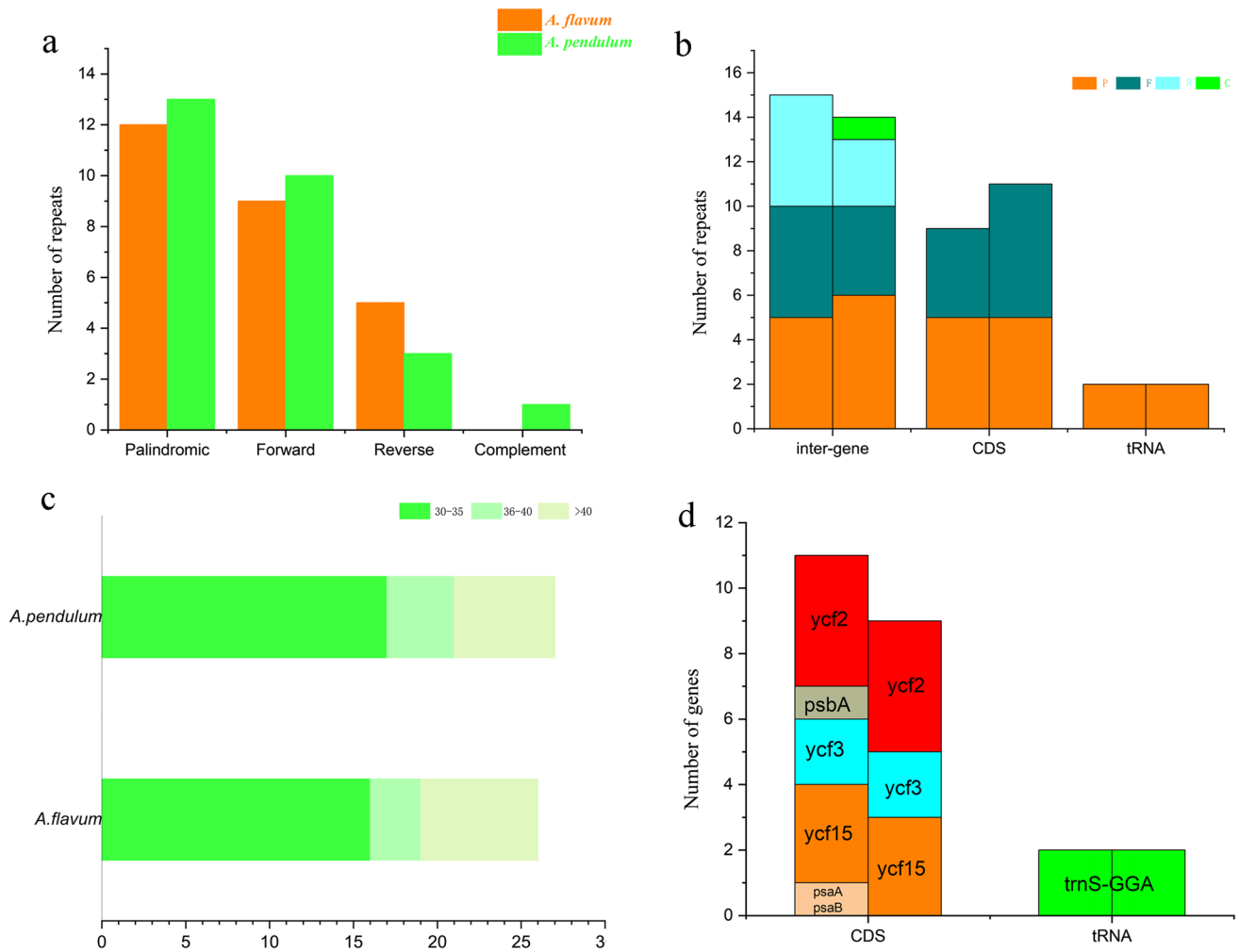


Fig. 2 Analyses of large repeats sequences in *A. pendulum* and *A. flavum*. **a** The number of four types of repeats. **b** Presence of type of repeats in inter-gene, CDS(coding sequence) and tRNA regions of *A. flavum* and *A. pendulum*: P (palindromic), F (Forward), R (Reverse)

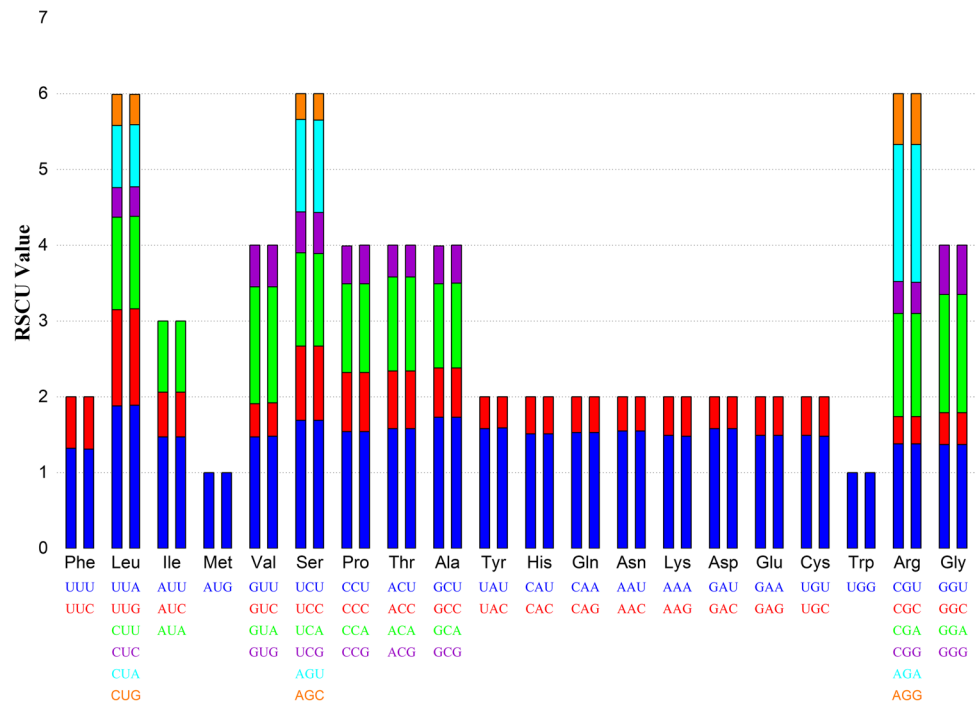
and C (Complement). **c** Frequency of four repeats by length. **d** Four type of repeats in gene of CDS and tRNA regions: *A. pendulum* (left) and *A. flavum* (right)

repeats, five reverse repeats. None complement repeats, only one complement repeat were detected in the *A. pendulum*. (Fig. 2a). Four types of repeats were abundant in the inter-gene region (Fig. 2b). The size of palindromic repeats in the two *Aconitum* species all ranged from 30 to 72 bp. Forward repeats ranged from 30 to 53 bp in *A. flavum* and from 30 to 52 in *A. pendulum*, reverse repeats ranged from 30 to 34 bp in *A. pendulum* and from 33 to 34 bp in *A. flavum* (Fig. 2c). In the two *Aconitum* species, two palindromic repeats (*trnS-GGA*) are all located in tRNA region. There are 4, 2, and 3 repeats were found in *ycf2*, *ycf3* and *ycf15* protein-coding genes. Furthermore, one repeat in protein-coding genes (*psaB*, *psaA* and *psbA*) only occurred in the plastome of *A. pendulum* (Fig. 2d).

Codon usage analysis

Seventy-eight protein-coding genes of *A. pendulum* and *A. flavum* plastome contained 61 types of codons and 20 types of amino acids (Fig. 3). The number of codons ranged from 65 to 939 (*A. flavum*) and 66 to 945 (*A. pendulum*). Among the 20 amino acids in *A. flavum* and *A. pendulum*, isoleucine was the most abundant amino acid, with 939 and 945, glutamic was the second abundant amino acid, with 869 and 871, while cysteine was the least, with 65 and 66. RSCU values of the 61 codons in the two *Aconitum* with 29 codons were greater than 1, whereas the A/U contents at the third codon position were about 49.2% and the G/C contents about 50.8% (Table S4). There was almost no difference between the two *Aconitum* species in RSCU values.

Fig. 3 Codon distribution of 20 amino acids in 79 protein-coding genes of the chloroplast genomes of *A. flavum* and *A. pendulum*



Comparative analysis of Plastomes

In our study, of the eight of Sect. *Aconitum* species, presence of Ser. *Brachypoda* (*A. brachypodum*, *Apsilochorema coreanum*, *A. flavum*, and *A. pendulum*), Ser. *Ambigua* (*A. delavayi* Franch.), Ser. *Tangutica* (*Aconitum tanguticum* (Maxim.) Stapf), Ser. *Volubilia* (*Aconitum carmichaelii* Debeaux) and Ser. *Stylosa* (*Aconitum contortum* Finet et Gagnep.) exhibited the same pattern in content and the number of genes in IR/LSC and IR/SSC boundary regions (Fig. 4). The sizes of IRs of *A. pendulum* and *A. flavum* all with 26,216 bp in length. The longest IRs sizes were *A. coreanum* (26,261 bp) with 67 bp length than the shortest (*A. brachypodum*: 26,149 bp). Except for *ndhF* gene, *A. pendulum* and *A. flavum*, including *rps19*, *rpl2*, *ycf1* and *trnH* established the same gene length and distance from IR/LSC and IR/SSC boundary. The *rps19* gene in the two *Aconitum* species all located in the LSC region and extended 3 bp in the IRb region, the longest extended was *A. tanguticum* with 58 bp in the IRb region. The *ndhF* and *trnH* genes of the eight species are all located in SSC and LSC regions. The ψ *ycf1* pseudogene located in IRb region and the length ranged from 1259 to 1294 bp, the *ycf1* gene spanned SSC/IRA border, between 3992 to 4090 bp in the SSC region and 1259 to 1354 bp in the IRA region.

All the published plastomes of Ser. *Brachypoda* (*Aconitum*) species including *A. brachypodum* (NC_041579), *A. coreanum* (NC_013421), *A. flavum*, and *A. pendulum* were compared using mVISTA, with the annotation of *A. flavum* MW839582 as the reference (Fig. 5). There was less

divergence in coding regions than non-coding regions showing more conserved in protein-coding regions. Large single copy (LSC) and small single copy (SSC) had higher genetic variability than inverted repeats regions (IR). In the coding regions, *rpoC2*, *rpoA* and *ycf1* were the most varied regions. In the intergenic regions, *matK-trnQ-UUG*, *atpH-atpI*, *petN-trnD-GUC*, *trnD-GUC-trnY-GUA*, *trnT-GGU-psbD*, *trnT-UGU-trnL-UAA*, *psbE-petL*, *ndhF-trnL-UAG*, *ccsA-ndhD* were higher diverged regions. Furthermore, four individuals of *A. flavum* and *A. pendulum* were compared, with *A. flavum* MW839582 and *A. pendulum* MW839581 as the reference (Fig. S1, Fig. S2). Most of the variations were found in intergenetic region region, such as *matK-trnQ-UUG*, *atpH-atpI*, *petN-psbM*, *psbM-trnD-GUC*, *trnT-GGU-psbD*, *petA-psbJ*, *psbE-petL*, *trnP-UGG-psbJ*, *rps18-rpl20*, *ycf1-ndhF*, *ndhF-trnL-UAA*, *ccsA-ndhD* and *ndhG-ndhI*. In the protein-coding region, *rpoC2*, *petB*, *rpoA*, *rpl16*, and *ycf1* were more divergent.

Plastome markers are widely used in phylogenetic analysis at the interspecies level. We further compared the divergent hotspots regions of 78 coding genes (Fig. 6a) and 46 intergenic non-coding genes (Fig. 6b) shared by 30 individuals of 17 *Aconitum* species by DnaSP v6. The coding regions were more conserved than intergenic regions, consistent with the mVISTA results. In the non-coding regions, the different individuals of *A. flavum* and *A. pendulum* all established markedly variation, only *atpB-rbcL*, *petB-petD*, *psaI-ycf4*, *trnM-CAU-atpE*, *trnN-GUU-trnR-ACG*, *trnR-ACG-trnA-UGC*, *trnS-GGA-rps4*, *ycf3-trnS-GGA* and *ycf15-trnL-CAA* conserved in the two *Aconitum* species. In the coding region,

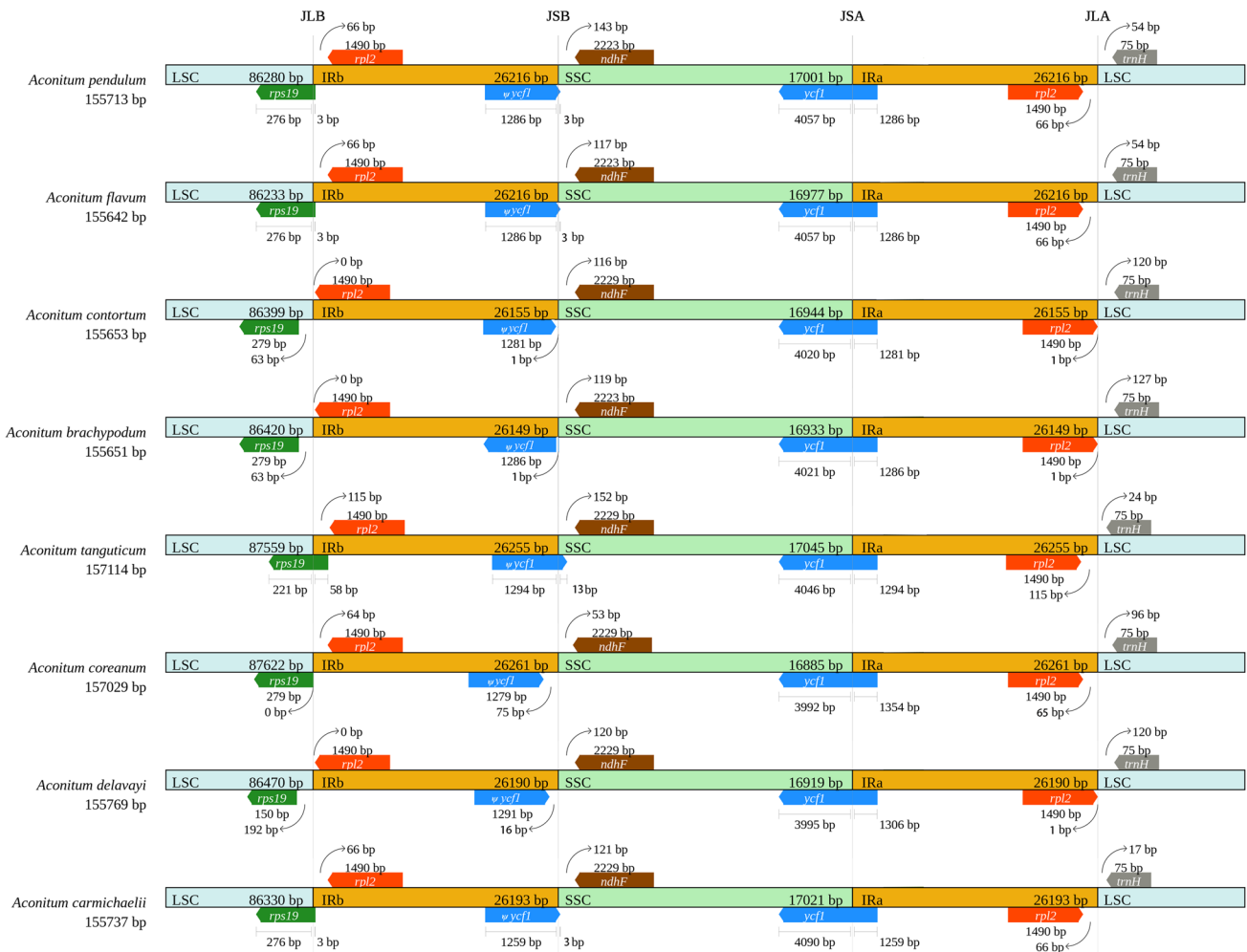


Fig. 4 Comparisons of LSC, SSC, and IR region borders among the eight *Aconitum* species

rpl20 and *rpoC1* were more divergent in intraspecies of *A. flavum* and *A. pendulum*, *ycf15*, with the highest variation among 17 *Aconitum* species. *ycf1* gene in our study with lower pi value, we also used *ycf1* gene to construct ML tree of the 17 *Aconitum* species (Fig. S3). It has low bootstrap values to solve the relationships of *A. flavum* and *A. pendulum*. Moreover, the *A. coreanum* KU318669 was separated from *A. coreanum* MN400660 and *A. coreanum* NC031421.

Phylogenetic analysis

Seventy-three protein-coding genes and cpDNA were used to construct ML and BI trees (Fig. 7). In our protein-coding genes tree results, Ser. *Tangutica* and Sect. *Paraconitum* grouped a single clade and had bootstrap values of 100%. In Ser. *Volubilia*, *A. carmichaelii*, *A. kusnezoffii*, *A. monanthum* Nakai, and *A. jaluense* Kom. formed a monophyletic clade with 100% bootstrap value or Bayesian posterior probability, and *A. vilmorinianum* Kom., *A. hemsleyanum*

Pritz., *A. episcopale* Leveille were cluster to Ser. *Ambigua* (*A. delavayi*). *A. episcopale* was sister to *A. delavayi*. Ser. *Brachypoda* were not clustered monophyletically. Three accessions of *A. coreanum* were clustered in a single branch. *A. pendulum*, *A. flavum* and *A. brachypodium* gathered in one clad, implying the closely-related relationship of the three species. *A. flavum* and *A. pendulum* were gathered in one clade. *A. flavum* MW839579 and *A. pendulum* MW839578 collected from Maqin, Qinghai Province clustered into one clade with the bootstrap value of 98% and 100% Bayesian posterior probability. *A. flavum* MW839582 and *A. pendulum* MW839577 collected from Zhiduo and Dari gathered in one clustered with bootstrap values or Bayesian posterior probability $\geq 99\%$.

Six commonly cpDNA regions (*atpB*, *matK*, *ndhF*, *rbcL*, *rps4*, *atpB-rbcL*) were combined and used to construct ML tree (Fig. 8f). *A. flavum*, *A. pendulum*, and *A. brachypodium* clustered into one branch, *A. flavum* and *A. pendulum* are closely related, consistent with the result of

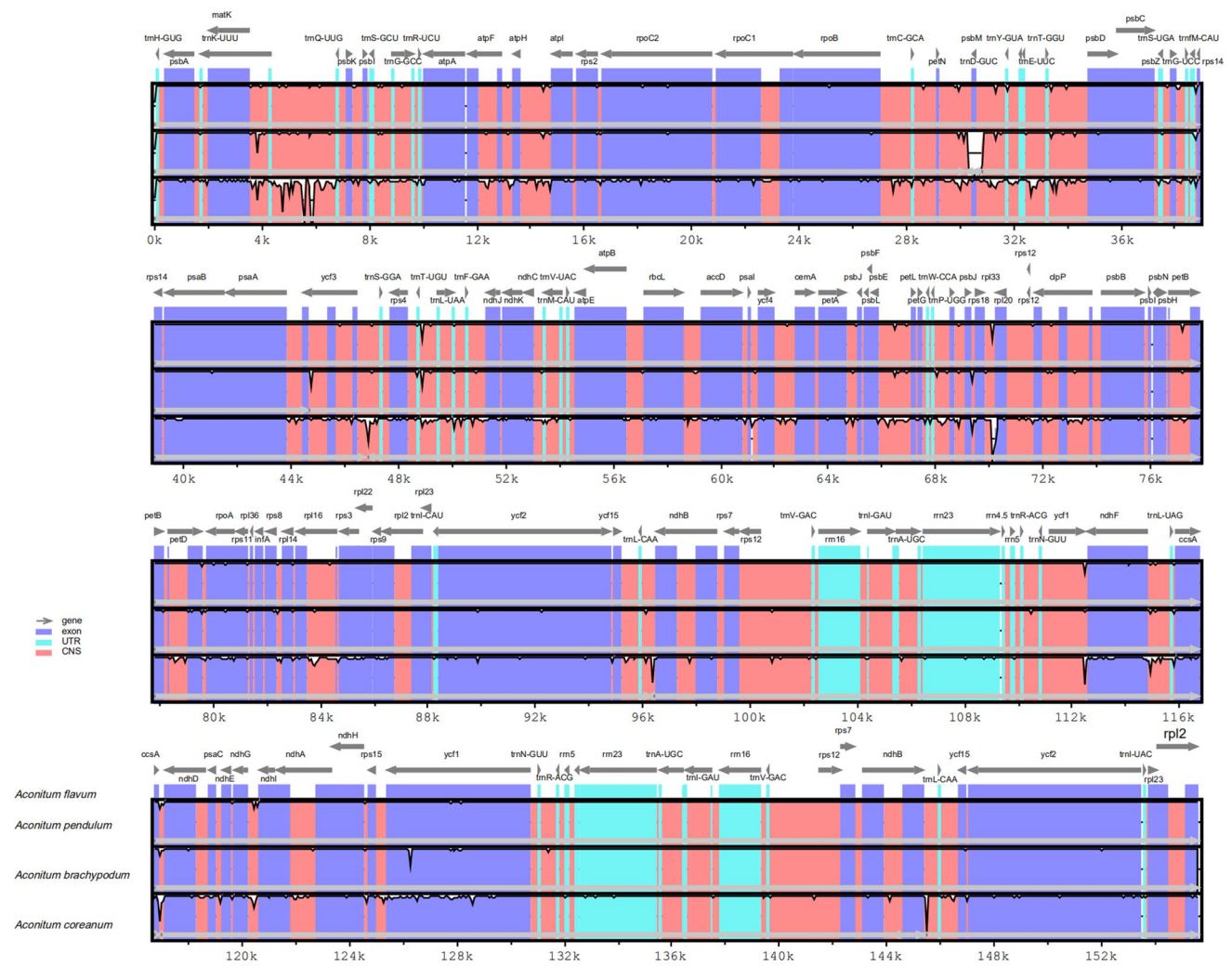


Fig. 5 Comparison of *Ser. Brachypoda* chloroplast genome using mVISTA and *A. flavum* as a reference. Blue represents coding regions, and red represents non-coding regions

73 protein-coding genes. But most of the nodes with much lower bootstrap values than based on the protein-coding genes. *A. coreanum* clustered with *Aconitum longecassidatum* NaKai and *A. sinomontanum* with 100% bootstrap values, inconsistent with prior research and our protein-coding sequences results. We also used highly variable regions ($pi > 0.2$) of plastome, which was found in our study to construct ML tree (Fig. 8a-e), including *atpB_rbcL*, *psaI_ycf4*, *trnR-ACG_trnA-UGC*, *ycf3_trnS-GGA*, and *ycf15_trnL-CAA*, but most of them with low bootstrap values in solving the phylogenetic relationships of *A. flavum* and *A. pendulum*.

Discussion

The plastome of *A. flavum* and *A. pendulum* shared a highly similar structure in genome size, gene content, and number. Still, the LSC region has more variation in different

individuals than SSC and IR regions. Moreover, the variation of LSC region was demonstrated mainly accounted for the plastomes difference (Chen et al. 2017). The GC content of *A. flavum* and *A. pendulum* was 38.1%, which were closed to that reported for other *Aconitum* plastomes (Li et al. 2020; Lim et al. 2020). Plastome variation in the intraspecies level of *A. flavum* and *A. pendulum* has a slight difference, also reported in *A. coreanum*, *A. jaluense*, and *A. brachypodum* (Kim et al. 2019).

11 and 9 long repeat sequences were detected in the two *Aconitum* species. It was also detected in protein-coding genes, such as *ycf2* gene, long repeat sequences in *ycf2* gene have also appeared in gene *Camellia* (Li et al. 2021). *A. flavum* and *A. pendulum* have different numbers of long repeat sequences, implying a slight difference in plastomes.

In the process of evolution, species will form a set of codons that use patterns to adapt to themselves. The similarity of codon preference indicates that species have similar

Fig. 6 Comparative analysis of the nucleotide variability (pi) values of the 17 *Aconitum* species. **a** intergenetic region, **b** coding region

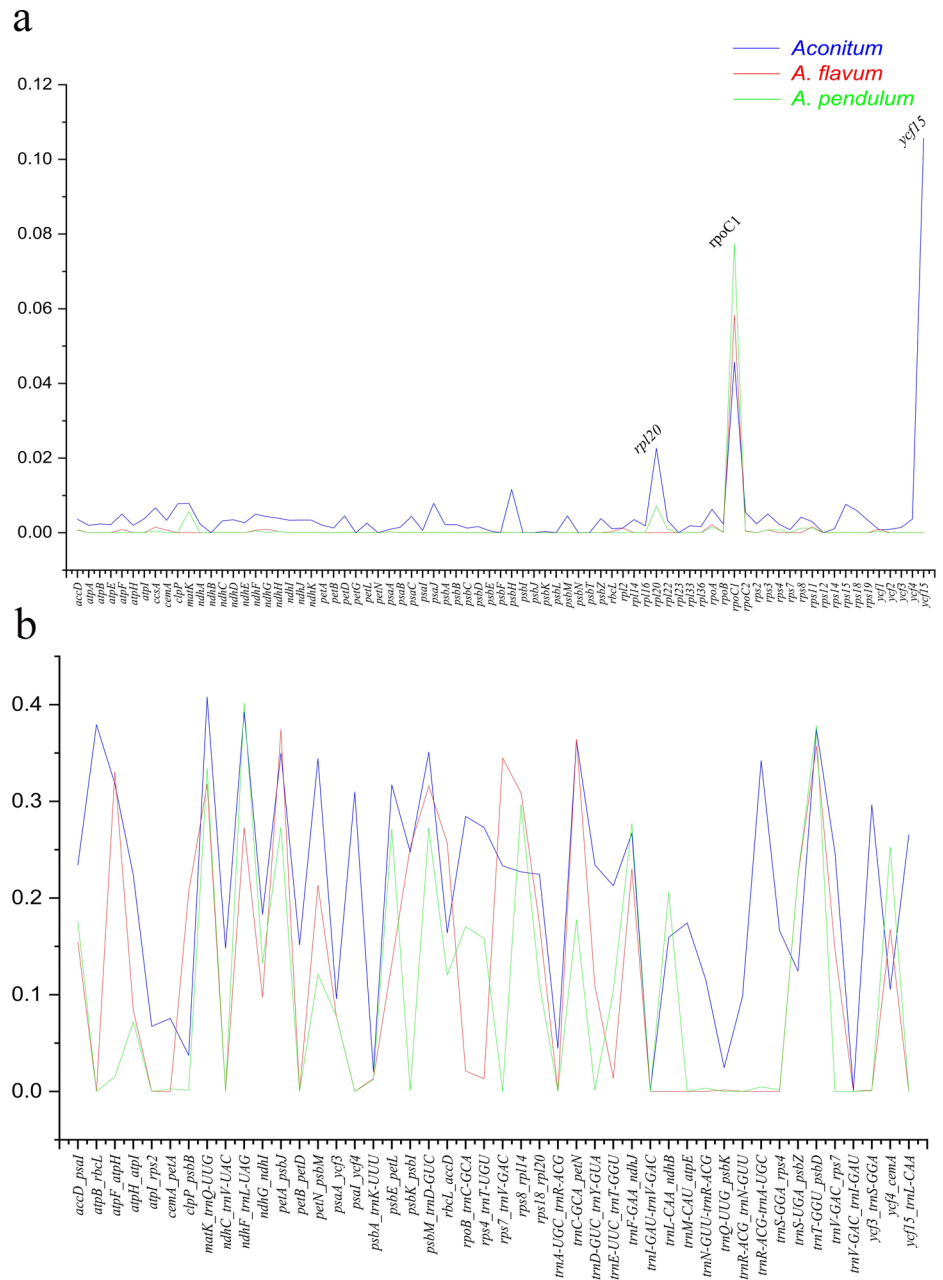


Fig. 7 Phylogeny of 17 *Aconitum* species with Maximum likelihood (ML, right) and Bayesian inference (BI, left) methods based on 73 shared protein-coding genes

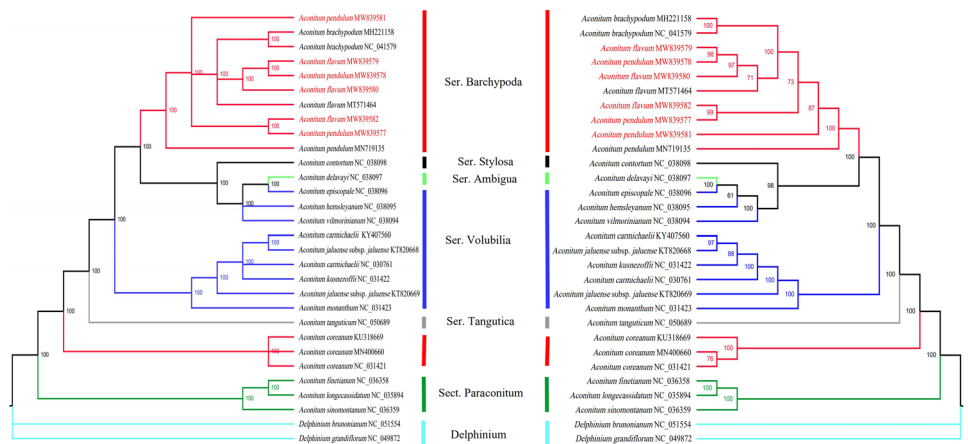
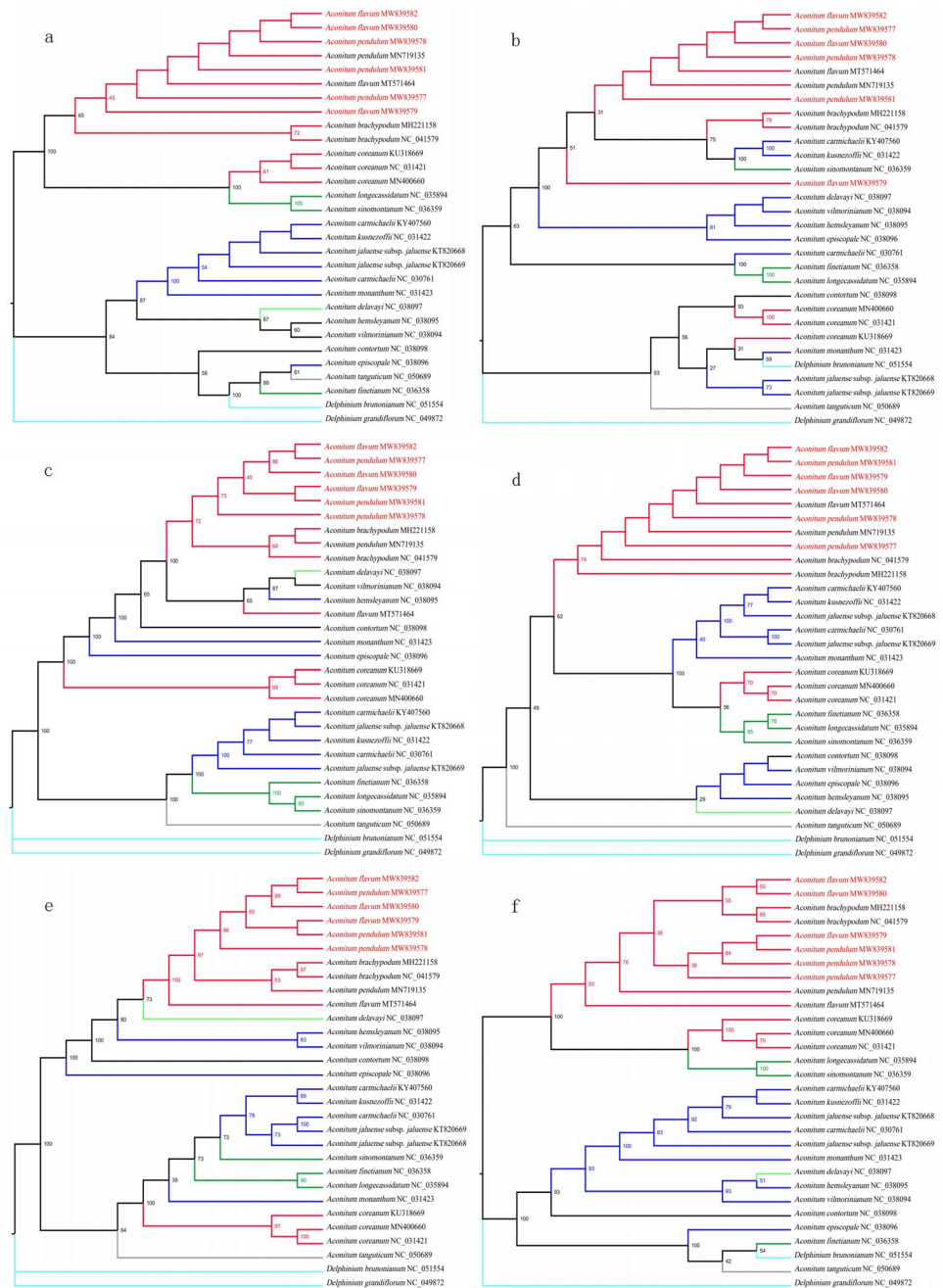


Fig. 8 Cladograms using the Maximum likelihood (ML) methods. a ML tree based on *atpB_rbcL*. b ML tree based on *psaI_ycf4*. c ML tree based on *ycf3_trnS-GGA*. d ML tree based on *trnR-ACG_trnA-UGC*. e ML tree based on the concatenation of *atpB_rbcL*, *psaI_ycf4*, *ycf3_trnS-GGA*, and *trnR-ACG_trnA-UGC*. (f) ML tree based on the concatenation of common cpDNA regions (*atpB*, *matK*, *ndhF*, *rbcL*, *rps4*, *atpB_rbcL*)



living environments or evolutionary histories. In our codon usage analysis, the G/C contents are abundant in the third codon position (50.8%), which is different from other species which enrich A/T at the third codon position (Fang et al. 2020). There was almost no difference between the two *Aconitum* species in RSCU values, which exhibited a similar pattern in other closely related species (Liang et al. 2020).

The contraction and expansion of IR caused the difference in plastome sizes (Hong et al. 2017), with slight variation among different species (Zhao and Zhu 2020). *Ser. Brachypoda* (*A. brachypodum*, *A. coreanum*, *A. flavum*, and

A. pendulum), *Ser. Ambigua* (*A. delavayi*), *Ser. Tangutica* (*A. tanguticum*), *Ser. Volubilia* (*A. carmichaelii*) and *Ser. Stylosa* (*A. contortum*) exhibited the same pattern in content and the number of genes in IR/LSC and IR/SSC boundary regions (Kong et al. 2013). Except for *ndhF* gene, *A. pendulum* and *A. flavum* established the same genes length and distance from IR/LSC and IR/SSC boundary, identical to the genus *Paeonia* (*Paeonia jishanensis* T. Hong & W. Z. Zhao and *Paeonia qiu* Y. L. Pei & D. Y. Hong; Wu et al. 2020).

Compared with other *Aconitum* species, protein-coding regions were more conserved than non-coding. And *rpoC2*,

rpoA, and *ycf1* were the most varied regions (Sobreiro et al. 2020). Plastome in intraspecies level has a slight difference. Prior research implied 12 plastomes of *Ricinus communis* L. owed largely conserved in plastome structure (Muraguri et al. 2020), which differs from our results. Furthermore, climatic variation may be the main reason for triggered genomic variation for four individuals of *A. flavum* and *A. pendulum* from different locations (Cuevas et al. 2021). Moreover, *ycf1* is a core barcode of land plants (Dong et al. 2015). Nucleotide diversity calculated in six *Arabidopsis* species, *trnL/trnF* showed significantly high pi values (Park et al. 2020), which differed from our result. Some protein-coding genes and intergenic regions have higher varied intraspecies than interspecies levels. Those variation genes may be suitable for population genetic analyses.

Phylogeny of *Aconitum* has been revealed based on nrDNA regions (internal transcribed spacer ITS, external transcribed spacer, ETS), cpDNA region (*ndhF-trnL*, *psbA-trnH*, *psbD-trnT* and *trnT-L*), Amplified fragment length polymorphism (AFLP), and the complete plastome (Kita and Ito 2000; Mitka et al. 2015; Liu et al. 2020; Wang and Li 2020). Those results were insufficient to resolve the phylogenetic relationships among the two species. The complete plastome has successfully solved the phylogenetic relationships of 6 morphology similarity species in genus *Atractylodes*, which prior researches used several chloroplast markers and have poor results (Wang et al. 2021). *A. flavum* and *A. pendulum* also have similar morphologic features. The phylogenetic relationships between the two species were also controversial. The plastome may bring dawn to resolve the systematic relationships of *A. flavum* and *A. pendulum*. Furthermore, prior research demonstrated that the same species from *Aconitum* (*A. carmichaelii*, *A. jaluense*, *A. japonicum*, and *A. kusnezoffii*) having different accessions did not cluster monophyletically, which may result from different ploidy within the species (Park et al. 2017; Kim et al. 2019). In this study, the two *Aconitum* (*A. pendulum* and *A. flavum*) were diploidy. To reduce the influence of polyploidy, we selected six individuals of the two species from six populations. In our phylogenetic tree, *A. episcopale* was sister to *A. delavayi*, consistent with prior results that *Ser. volubilia* were not monophyly (Meng et al. 2018). *A. coreanum* was separated from the rest of species in *Ser. Brachypoda*, consistent with the analysis of diterpenoid alkaloid of *A. coreanum*, *Ser. Brachypoda* was not monophyletic (Xiao et al. 2006). *A. flavum* and *A. pendulum* were gathered in one clade, different from the resulting from ITS (Luo et al. 2005). The four individuals of *A. pendulum* and *A. flavum* from different locations did not cluster together. On the one hand, it may be affected by geographical and ecological factors, which were also occurred in the speciation of the genus *Chrysanthemum* (Liu et al. 2012; Tyagi et al. 2020). The two species had racemose inflorescence and the

same florescence. The pollinating agent of the two species may be by bumblebees and/or wind, which was reported in other *Aconitum* species (Wang et al. 2009). Moreover, hybridization was not rare in *Aconitum* species, such as *A. firmum* Rchb. × *A. variegatum* L. and *Aconitum lasiocarpum* (Rchb.) Gáyer × *A. variegatum* L. (Sutkowska et al. 2017). Overlapping geographical distribution, hybridization, and gene flow could affect the interspecific boundaries of *A. pendulum* and *A. flavum* (Petit and Excoffier 2009). As discussed above, *A. flavum* and *A. pendulum* have similar morphological characteristics, species distribution, highly identical plastome structure, and indistinct phylogenetic relationship. Further research for the two species is necessary, such as population genetic study, to reveal they are the same or two distinct species.

The tree constructed by cpDNA regions had much lower bootstrap values than the protein-coding genes, which also appeared in other species (Wu et al. 2020). The protein-coding genes have higher bootstrap values in solving closely related species than highly varied regions, mainly resulting from DNA barcoding and highly variation regions with limited informative sites provided (Xu et al. 2015; Wu et al. 2020) and highly divergent in intraspecies level. DNA barcoding regions have different evolutionary rates among other taxa. For example, the *ycf1* gene in Rosaceae and genus *Ilex* had high variations (Yang et al. 2020; Kong et al. 2021), but our research had a low pi value.

Conclusion

The plastomes of *A. flavum* and *A. pendulum* shared a highly similar genome size, gene content and number, GC content, and IR contraction and expansion. Four types of large repeats mainly exist in intergenic regions, and codon usage was also analyzed. Compared with other *Aconitum* species, protein-coding regions were more conserved than non-coding. *rpoC1* and *rpl20* have higher variation in intraspecies levels, which could be helpful for population genetic analyses. Furthermore, intergenic regions were more divergent in intraspecies of *A. flavum* and *A. pendulum*. A total of 9 hotspots were identified and valuable for species identification. The phylogenetic trees were carried out using protein-coding genes and the cpDNA region. In our protein-coding tree result, *A. flavum* and *A. pendulum* were closely related and highly bootstrap value or Bayesian posterior probability. *A. flavum* and *A. pendulum* have similar morphological characteristics, species distribution, highly identical plastome structure, and indistinct phylogenetic relationship. Further research for the two species is necessary, such as population genetic study, to reveal they are the same or two distinct species.

Supplementary Information The online version contains supplementary material available at <https://doi.org/10.1007/s11756-021-00969-6>.

Authors' contributions Faqi Zhang and Shilong Chen conceived the idea and led the experiment. Qiang Li, Jingya Yu and Mingze Xia worked on the experimental proposal, the experimental design, and the analysis of the experimental results. Qiang Li wrote the first draft of the paper. All the authors contributed to the final version of the manuscript.

Funding This research was partially supported by the Second Tibetan Plateau Scientific Expedition and Research (STEP) program (2019QZKK05020102), Key Research and Development, transformative Program of Qinghai Province (2021-HZ-807), the Strategic Priority Research Program of the Chinese Academy of Sciences (XDA2005020405), Chinese Academy of Sciences -People's Government of Qinghai Province on Sanjiangyuan National Park (LHZX-2021-04), Construction Project for Innovation Platform of Qinghai province (2017-ZJ-Y14 & 2021-ZJ-Y05).

Data availability The DNA sequences were submitted to GenBank under the accession numbers in supplementary information Table S1.

Code availability Not application.

Declarations

Ethical approval Before collecting the samples, oral permission was obtained from the local government after applying with introduction letters of Northwest Institute of Plateau Biology, Chinese Academy of Sciences.

Consent to participate Not application.

Consent for publication Not application.

Conflicts of interest/competing interests The authors declare that they have no conflict of interest.

References

- Bankevich A, Nurk S, Antipov D, Gurevich AA, Dvorkin M, Kulikov AS, Lesin VM, Nikolenko SI, Pham S, Prjibelski AD, Pyshkin AV, Sirotkin AV, Vyahhi N, Tesler G, Alekseyev MA, Pevzner PA (2012) SPAdes: a new genome assembly algorithm and its applications to single-cell sequencing. *J Comput Biol* 19:455–477. <https://doi.org/10.1089/cmb.2012.0021>
- Chen X, Zhou J, Cui Y, Wang Y, Duan B, Yao H (2018) Identification of *Ligularia* herbs using the complete chloroplast genome as a super-barcode. *Front Pharmacol* 9:1–11. <https://doi.org/10.3389/fphar.2018.00695>
- Chen Z, Grover CE, Li P, Wang Y, Nie H, Zhao Y, Wang M, Liu F, Zhou Z, Wang X, Cai X, Wang K, Wendel JF, Hua J (2017) Molecular evolution of the plastid genome during diversification of the *cotton* genus. *Mol Phylogenet Evol* 112:268–276. <https://doi.org/10.1016/j.ympev.2017.04.014>
- Cuevas A, Ravinet M, Sætre GP, Eroukmanoff F (2021) Intraspecific genomic variation and local adaptation in a young hybrid species. *Mol Ecol* 30:791–809. <https://doi.org/10.1111/mec.15760>
- El-Shazly M, Tai CJ, Wu TY, Csupor D, Hohmann J, Chang FR, Wu YC (2016) Use, history, and liquid chromatography/mass spectrometry chemical analysis of *Aconitum*. *J Food Drug Anal* 24:29–45. <https://doi.org/10.1016/j.jfda.2015.09.001>
- Fang J, Lin A, Yuan X, Chen Y, He W, Huang J, Zhang X, Lin G, Zhang J, Xue T (2020) The complete chloroplast genome of *Isochrasis galbana* and comparison with related haptophyte species. *Algal Res* 50:101989. <https://doi.org/10.1016/j.algal.2020.101989>
- Frazer KA, Pachter L, Poliakov A, Rubin EM, Dubchak I (2004) VISTA: computational tools for comparative genomics. *Nucleic Acids Res* 32:273–279. <https://doi.org/10.1093/nar/gkh458>
- Greiner S, Lehwark P, Bock R (2019) OrganellarGenomeDRAW (OGDRAW) version 1.3.1: expanded toolkit for the graphical visualization of organellar genomes. *Nucleic Acids Res* 47:W59–W64. <https://doi.org/10.1093/nar/gkz238>
- Hong SY, Cheon KS, Yoo KO, Lee HO, Cho KS, Suh JT, Kim SJ, Nam JH, Sohn HB, Kim YH (2017) Complete chloroplast genome sequences and comparative analysis of *Chenopodium quinoa* and *C. Album*. *Front Plant Sci* 8:1–12. <https://doi.org/10.3389/fpls.2017.01696>
- Jabbour F, Renner SS (2012) A phylogeny of Delphinieae (*Ranunculaceae*) shows that *Aconitum* is nested within *Delphinium* and that Late Miocene transitions to long life cycles in the Himalayas and Southwest China coincide with bursts in diversification. *Mol Phylogenet Evol* 62:928–942. <https://doi.org/10.1016/j.ympev.2011.12.005>
- Jiang K, Miao L, Wang Z, Ni Z, Hu C, Zeng X, Huang W (2020) Chloroplast genome analysis of two medicinal *Coelogyne* spp. (*Orchidaceae*) Shed Light on the Genetic Information, Comparative Genomics, and Species Identification. *Plants* 9:1332. <https://doi.org/10.3390/plants9101332>
- Jin JJ, Bin YW, Yang JB, Song Y, DePamphilis CW, Yi TS, Li DZ (2020) GetOrganelle: a fast and versatile toolkit for accurate de novo assembly of organelle genomes. *Genome Biol* 21:241. <https://doi.org/10.1101/256479>
- Katoh K, Rozewicki J, Yamada KD (2019) MAFFT online service: multiple sequence alignment, interactive sequence choice and visualization. *Brief Bioinform* 20:1160–1166. <https://doi.org/10.1093/bib/bbx108>
- Kim Y, Yi JS, Min J, Xi H, Kim DY, Son J, Park J, Jeon JI (2019) The complete chloroplast genome of *Aconitum coreanum* (H. Lév.) Rapaics (*Ranunculaceae*). *Mitochondrial DNA Part B Resour* 4:3404–3406. <https://doi.org/10.1080/23802359.2019.1674213>
- Kita Y, Ito M (2000) Nuclear ribosomal ITS sequences and phylogeny in east Asian *Aconitum* subgenus *Aconitum* (*Ranunculaceae*), with special reference to extensive polymorphism in individual plants. *Plant Syst Evol* 225:1–13. <https://doi.org/10.1007/BF00985455>
- Kita Y, Ueda K, Kadota Y (1995) Molecular phylogeny and evolution of the Asian *Aconitum* subgenus *Aconitum* (*Ranunculaceae*). *J Plant Res* 108:429–442. <https://doi.org/10.1007/BF02344231>
- Kong HH, Gao Q, Luo Y, Yang QE (2013) Seed morphology in some Chinese species of *Aconitum* (*Ranunculaceae*) and its systematic implications. *Plant Divers Resour* 35:241–252
- Kumar S, Stecher G, Li M, Knyaz C, Tamura K (2018) MEGA X: molecular evolutionary genetics analysis across computing platforms. *Mol Biol Evol* 35:1547–1549. <https://doi.org/10.1093/molbev/msy096>
- Kurtz S, Choudhuri JV, Ohlebusch E, Schleiermacher C, Stoye J, Giegerich R (2001) REPuter: the manifold applications of repeat analysis on a genomic scale. *Nucleic Acids Res* 29:4633–4642. <https://doi.org/10.1093/nar/29.22.4633>
- Li L, Hu Y, He M, Zhang B, Wu W, Cai P, Huo D, Hong Y (2021) Comparative chloroplast genomes: insights into the evolution of the chloroplast genome of *Camellia sinensis* and the phylogeny of *Camellia*. *BMC Genomics* 22(138). <https://doi.org/10.1186/s12864-021-07427-2>

- Li L, Kadota Y (2001) *Aconitum* L. In: Wu Z, Raven P (eds) Flora of China. Science Press/Missouri Botanical Garden, Beijing, pp 149–222
- Li Q, Li X, Qieyang R, Nima C, Dongzhi D, Duojie GX (2020) Characterization of the complete chloroplast genome of the Tangut monkshood *Aconitum tanguticum* (Ranunculales: Ranunculaceae). Mitochondrial DNA Part B Resour 5:2306–2307. <https://doi.org/10.1080/23802359.2020.1773338>
- Li Y, Meng Y, Shen S, Wang Y (2012) Karyological studies of *Aconitum brachypodum* and related species. Cytologia (Tokyo) 77:491–498. <https://doi.org/10.1508/cytologia.77.491>
- Liang H, Zhang Y, Deng J, Gao G, Ding C, Zhang L, Yang R (2020) The complete chloroplast genome sequences of 14 *Curcuma* species: insights into genome evolution and phylogenetic relationships within Zingiberales. Front Genet 11:1–17. <https://doi.org/10.3389/fgene.2020.00802>
- Lim CE, Ryul BK, Lee JD, Jung KD, Noh TK, Lee BY (2020) The complete chloroplast genome of *Aconitum puchonroenicum* Uyeki & Sakata (Ranunculaceae), a rare endemic species in Korea. Mitochondrial DNA Part B Resour 5:1284–1285. <https://doi.org/10.1080/23802359.2020.1734497>
- Liu PL, Wan Q, Guo YP, Yang J, Rao GY (2012) Phylogeny of the genus *Chrysanthemum* L.: evidence from single-copy nuclear gene and chloroplast DNA sequences. PLoS One 7(11):e48970. <https://doi.org/10.1371/journal.pone.0048970>
- Liu Y, Yu S, You F (2020) Characterization of the complete chloroplast genome of *Aconitum flavum* (Ranunculaceae). Mitochondrial DNA Part B Resour 5:3000–3001. <https://doi.org/10.1080/23802359.2020.1787894>
- Luo Y, Zhang FM, Yang QE (2005) Phylogeny of *Aconitum* subgenus *Aconitum* (Ranunculaceae) inferred from ITS sequences. Plant Syst Evol 252:11–25. <https://doi.org/10.1007/s00606-004-0257-5>
- Ma L, Gu R, Tang L, Chen ZE, Di R, Long C (2015) Important poisonous plants in Tibetan ethnomedicine. Toxins (Basel) 7:138–155. <https://doi.org/10.3390/toxins7010138>
- Meng J, Li X, Li H, Yang J, Wang H, He J (2018) Comparative analysis of the complete chloroplast genomes of four *Aconitum* medicinal species. Molecules 23:5–9. <https://doi.org/10.3390/molecules23051015>
- Minh BQ, Schmidt HA, Chernomor O, Schrempf D, Woodhams MD, Von Haeseler A, Lanfear R, Teeling E (2020) IQ-TREE 2: new models and efficient methods for phylogenetic inference in the genomic era. Mol Biol Evol 37:1530–1534. <https://doi.org/10.1093/molbev/msaa015>
- Mitka J, Boroń P, Wróblewska A, Bąba W (2015) AFLP analysis reveals infraspecific phylogenetic relationships and population genetic structure of two species of *Aconitum* in Central Europe. Acta Soc Bot Pol 84:267–276. <https://doi.org/10.5586/asbp.2015.012>
- Muraguri S, Xu W, Chapman M, Muchugi A, Oluwaniyi A, Oyebanji O, Liu A (2020) Intraspecific variation within Castor bean (*Ricinus communis* L.) based on chloroplast genomes. Ind Crop Prod 155(112779). <https://doi.org/10.1016/j.indcrop.2020.112779>
- Park I, Kim WJ, Yang S, Yeo SM, Li H, Moon BC (2017) The complete chloroplast genome sequence of *Aconitum coreanum* and *Aconitum carmichaelii* and comparative analysis with other *Aconitum* species. PLoS One 12(9):e0184257. <https://doi.org/10.1371/journal.pone.0184257>
- Park J, Xi H, Kim Y (2020) The complete chloroplast genome of *Arabidopsis thaliana* isolated in Korea (Brassicaceae): an investigation of intraspecific variations of the chloroplast genome of Korean *a. thaliana*. Int J Genomics 2020:3236461. <https://doi.org/10.1155/2020/3236461>
- Petit RJ, Excoffier L (2009) Gene flow and species delimitation. Trends Ecol Evol 24:386–393. <https://doi.org/10.1016/j.tree.2009.02.011>
- Ronquist F, Teslenko M, Van Der Mark P, Ayres DL, Darling A, Höhna S, Larget B, Liu L, Suchard MA, Huelsenbeck JP (2012) MrBayes 3.2: efficient bayesian phylogenetic inference and model choice across a large model space. Syst Biol 61:539–542. <https://doi.org/10.1093/sysbio/sys029>
- Rozas J, Ferrer-Mata A, Sanchez-DelBarrio JC, Guirao-Rico S, Librado P, Ramos-Onsins SE, Sanchez-Gracia A (2017) DnaSP 6: DNA sequence polymorphism analysis of large data sets. Mol Biol Evol 34:3299–3302. <https://doi.org/10.1093/molbev/msx248>
- Salick J, Byg A, Amend A, Gunn B, Law W, Schmidt H (2006) Tibetan medicine plurality. Econ Bot 60:227–253
- Sataloff RT, Johns MM, Kost KM (2012) Clustering analysis of karyotype resemblance-near coefficient of 16 *Aconitum* L. species. Acta Agrestia Sin 20:352–357
- Sobreiro MB, Vieira LD, Nunes R, Novaes E, Coissac E, Silva-Junior OB, Grattapaglia D, Collevatti RG (2020) Chloroplast genome assembly of *Handroanthus impetiginosus*: comparative analysis and molecular evolution in Bignoniaceae. Planta 252:1–16. <https://doi.org/10.1007/s00425-020-03498-9>
- Sugiura M (1989) The chloroplast chromosomes in land plants. Annu Rev Cell Biol 5:51–70. <https://doi.org/10.1146/annurev.cb.05.110189.000411>
- Sutkowska A, Boroń P, Warzecha T, Dębowski J, Mitka J (2017) Hybridization and introgression among three *Aconitum* (Ranunculaceae) species of different ploidy levels in the Tatra Mountains (Western Carpathians). Plant Species Biol 32:292–303. <https://doi.org/10.1111/1442-1984.12162>
- Tamura M (1990) A new classification of the family Ranunculaceae I. Acta Phytotaxon Geobot 41:93–101
- Tillich M, Lehwark P, Pellizzer T, Ulbricht-Jones ES, Fischer A, Bock R, Greiner S (2017) GeSeq - versatile and accurate annotation of organelle genomes. Nucleic Acids Res 45:W6–W11. <https://doi.org/10.1093/nar/gkx391>
- Tyagi S, Jung JA, Kim JS, Won SY (2020) A comparative analysis of the complete chloroplast genomes of three *Chrysanthemum* boreale strains. PeerJ 2020:1–20. <https://doi.org/10.7717/peerj.9448>
- Wang B, Dong J, Ji J, Yuan J, Wang J, Wu J, Tan P, Liu Y (2016) Study on the alkaloids in Tibetan medicine *Aconitum pendulum* Busch by HPLC-MSn combined with column chromatography. J Chromatogr Sci 54:752–758. <https://doi.org/10.1093/chromsci/bmw002>
- Wang J, Meng XH, Chai T, Yang JL, Shi YP (2019) Diterpenoid alkaloids and one Lignan from the roots of *Aconitum pendulum* Busch. Nat Products Bioprospect 9:419–423. <https://doi.org/10.1007/s13659-019-00227-y>
- Wang L, Abbott RJ, Zheng W, Chen P, Wang Y, Liu J (2009) History and evolution of alpine plants endemic to the Qinghai-Tibetan plateau: *Aconitum gymnantrum* (Ranunculaceae). Mol Ecol 18:709–721. <https://doi.org/10.1111/j.1365-294X.2008.04055.x>
- Wang Y, Wang S, Liu Y, Yuan Q, Sun J, Guo L (2021) Chloroplast genome variation and phylogenetic relationships of *Atractylodes* species. BMC Genomics 22:1–12. <https://doi.org/10.1186/s12864-021-07394-8>
- Wang ZH, Li YQ (2020) Characterization of the complete chloroplast genome of *Aconitum pendulum* (Ranunculaceae), an endemic medicinal herb. Mitochondrial DNA Part B Resour 5:382–383. <https://doi.org/10.1080/23802359.2019.1703592>
- Wick RR, Schultz MB, Zobel J, Holt KE (2015) Bandage: interactive visualization of de novo genome assemblies. Bioinformatics 31:3350–3352. <https://doi.org/10.1093/bioinformatics/btv383>
- Wu L, Nie L, Xu Z, Li P, Wang Y, He C, Song J, Yao H (2020) Comparative and phylogenetic analysis of the complete chloroplast genomes of three *Paeonia* section Moutan species (Paeoniaceae). Front Genet 11:980. <https://doi.org/10.3389/fgene.2020.00980>
- Xiao PG, Wang FP, Gao F, Yan LP, Chen DL, Liu Y (2006) A pharmacophylogenetic study of *Aconitum* L. (Ranunculaceae) from

- China. Acta Phytotaxon Sin 44:1–46. <https://doi.org/10.1360/aps050046>
- Xu S, Li D, Li J, Xiang X, Jin W, Huang W, Jin X, Huang L (2015) Evaluation of the DNA barcodes in *Dendrobium* (Orchidaceae) from mainland Asia. PLoS One 10(1):e0115168. <https://doi.org/10.1371/journal.pone.0115168>
- Yang J, Kang GH, Pak JH, Kim SC (2020) Characterization and comparison of two complete plastomes of *Rosaceae* species (*Potentilla dickinsii* var. *glabrata* and *spiraea insularis*) endemic to Ulleung Island. Korea Int J Mol Sci 21:1–15. <https://doi.org/10.3390/ijms21144933>
- Yang Q (1994) A karyotype study of 15 species in the tribe Delphineae (Ranunculaceae) from China. J Syst Evol 34:39–47
- Zhang D, Gao F, Jakovlić I, Zou H, Zhang J, Li WX, Wang GT (2020) PhyloSuite: an integrated and scalable desktop platform for streamlined molecular sequence data management and evolutionary phylogenetics studies. Mol Ecol Resour 20:348–355. <https://doi.org/10.1111/1755-0998.13096>
- Zhao F, Chen YP, Salmaki Y, Drew BT, Wilson TC, Scheen AC, Celep F, Bräuchler C, Bendiksby M, Wang Q, Min DZ, Peng H, Olmstead RG, Li B, Xiang CL (2021) An updated tribal classification of *Lamiaceae* based on plastome phylogenomics. BMC Biol 19:1–27. <https://doi.org/10.1186/s12915-020-00931-z>
- Zhao XL, Zhu ZM (2020) Comparative genomics and phylogenetic analyses of *Christia vespertilionis* and *Urariopsis brevissima* in the tribe *Desmodieae* (Fabaceae: Papilionoideae) based on complete chloroplast genomes. Plants 9(9):1116. <https://doi.org/10.3390/plants9091116>

Publisher's note Springer Nature remains neutral with regard to jurisdictional claims in published maps and institutional affiliations.